



Investigation of the molecular dynamics of restricted water in wood by broadband dielectric measurements

S. Sudo^{1,*} , Y. Suzuki², F. Abe³, Y. Hori³, T. Nishi³, T. Kawaguchi³, H. Saito³, and S. Yagihara³

¹Department of Physics, Tokyo City University, Tokyo 158-8557, Japan

²Forestry and Forest Products Research Institute, Tsukuba, Ibaraki 305-8687, Japan

³Department of Physics, School of Science, Tokai University, Hiratsuka, Kanagawa 259-1292, Japan

Received: 1 June 2017

Accepted: 13 November 2017

Published online:

21 November 2017

© Springer Science+Business Media, LLC, part of Springer Nature 2017

ABSTRACT

Dielectric measurements are one of the most reliable techniques for investigating the molecular dynamics of water in moist materials. However, dielectric measurements of moist wood have not yet been carried out in a wide frequency range that can be used to evaluate the molecular dynamics of water in wood. We performed dielectric measurements of a deciduous tree, *Zelkova serrata*, along the fiber direction in the frequency range of 40 Hz to 10 GHz at room temperature around the fiber saturation point of wood to investigate the molecular dynamics of water in wood. Cole–Cole-type relaxation process reflecting the molecular dynamics of the water is observed in the GHz region. The water content dependences of the relaxation time and strength of this process are similar to those of the relaxation process of free water observed in polymer–water mixtures. However, the $\tau - \beta_{CC}$ diagram of this process markedly deviates from that of the relaxation process of free water in polymer–water mixtures. The molecular mechanism of this characteristic relaxation process is interpreted as the formation of the local structure of water restricted in the void spaces of wood. The water molecules adsorbed on the inner walls of the void spaces form a local structure, and the local structure grows in the length direction along the walls of the void spaces with increasing water content of wood. The molecular dynamics of these water molecules is strongly restricted between the inner walls of the void spaces and air spaces, and the strongly restricted molecular dynamics of the water leads to the characteristic relaxation process observed in the GHz region. We give molecular descriptions of the strongly restricted water adsorbed on the inner walls of the void spaces of wood around the fiber saturation point.

Address correspondence to E-mail: ssudo@tcu.ac.jp

Introduction

The microscopic environment of water in wood significantly affects the physical properties of the wood, such as the specific gravity, mechanical strength, and electrical conductivity. Thus, it is important to understand the microscopic environment of water in wood not only for theoretical studies, but also for industrial applications. In general, water in wood is roughly classified into two types called free water and bound water [1]. Free water exists in the intercellular spaces, vessels, and tracheids in wood, and these water molecules are transported relatively freely by the capillary force. Bound water exists in wood cell walls, which consist of an amorphous matrix of hemicelluloses and lignin. Bound water forms hydrogen bonds with the hydroxyl groups of hemicelluloses and lignin, and the dynamics of bound water is strongly restricted by these hydrogen bonds. Investigations of the molecular descriptions of water in wood have been performed by differential scanning calorimetry (DSC) [2, 3], nuclear magnetic resonance (NMR) [4, 5], near-infrared spectroscopy [6], dielectric spectroscopy [7–12], and theoretical approaches [13], and the water in wood has now been classified into more than two types based on the molecular dynamics of water reflecting the dipole interactions [2, 6, 13]. However, the molecular descriptions of these water molecules in detail have not been clear yet.

Dielectric spectroscopy is a technique used to observe the dielectric relaxation phenomena arising from the rotational dynamics of dipole moments. It is one of the most reliable techniques for investigating the molecular dynamics of water molecules in moist materials because water molecules have a large dipole moment. Furthermore, the dielectric relaxation spectrum obtained by dielectric measurements can be quantitatively expressed using relaxation parameters such as the relaxation strength, relaxation time, and relaxation time distribution. The relaxation strength reflects the number of dipole moments per unit volume, and the relaxation time reflects the time scale associated with the dynamical behavior of dipole moments. The relaxation time distribution is the shape parameter of the dielectric relaxation spectrum, and it reflects the heterogeneity of the dipole moment dynamics [14, 15]. Since the 1970s, dielectric measurements of fresh, chemically treated, and heat-

treated wood of various species have been performed in the kHz–MHz region, and the relaxation processes reflecting the motion of bound water [16–18], the reorientation of CH₂OH groups in cellulose [19], and the contribution of conductivity [7–10] have been observed. Recently, dielectric measurements of wood have been performed in the GHz region [20–24]. Mai et al. [20] evaluated the moisture content of wood from the dielectric constant measured using an electromagnetic signal at 1.26 GHz. Koubaa et al. [21] performed dielectric measurements of Canadian wood at frequencies of 0.4–2.47 GHz to evaluate the moisture content of wood. Tomppo et al. [22] performed dielectric measurements of *Pinus sylvestris* at the frequencies of 1 MHz to 1 GHz to evaluate the resin acid content of wood. Jördens et al. [23] performed terahertz time-domain spectroscopy measurements of a wood–plastic composite in the frequency range of 0.2 GHz to 1.0 THz to investigate the sorption of water in the composite material. However, dielectric measurements have not yet been carried out in a wide frequency range that can be used to evaluate the molecular dynamics of water in detail.

We have developed suitable dielectric measurement equipment and analytical methods to carry out measurements in a sufficiently high and wide frequency range. Time-domain reflectometry using flat-end coaxial electrodes is an effective dielectric measurement technique that obtains information on the molecular dynamics of water in moist materials [25–30]. The advantage of flat-end coaxial electrodes is that the dielectric measurement can be performed nondestructively up to 30 GHz [31]. We previously performed time-domain reflectometry measurements using flat-end coaxial electrodes in the frequency range of 100 Hz to 30 GHz for various moist materials, such as synthetic polymers, biopolymers, and cement [25–30, 32, 33]. We clarified that the molecular dynamics of the free and bound water as two different processes distinguished from those respective relaxation times. In the present work, we performed dielectric measurements of wood with various water contents in the fiber direction using flat-end coaxial electrodes in the frequency range of 40 Hz to 10 GHz at room temperature to clarify the molecular descriptions of water in wood. The relaxation process caused by the molecular dynamics of water was observed in the measured frequency range. The characteristic molecular dynamics of water

contributing to this process in wood is discussed on the basis of the results of the dielectric measurements.

Materials and methods

A deciduous tree used widely for building materials, *Zelkova serrata*, was used for the wood samples in this experiment. The age of the *Zelkova serrata* tree used in this experiment was 40 years. The trunk of the tree was cut at a height of 5 m above the ground, and the radius of the cut trunk was 5–20 cm. Wood samples were prepared by cutting the trunk into small cuboidal plates with dimensions of $2 \times 2 \times 1 \text{ cm}^3$ (radial, tangential, and longitudinal directions). Each sample was dried in a dry room at $20 \pm 3 \text{ }^\circ\text{C}$ with humidity less than 20% to prepare wood samples with various water contents. The longest drying period was 1 month. The index of the water content of each piece was evaluated as the weight of water per unit volume [g/cm^3], the so-called water density, given by

$$\rho_{\text{wat}} = \frac{w - w_0}{w} \rho_{\text{pw}} \tag{1}$$

Here, ρ_{pw} is the density of pure water ($\rho_{\text{pw}} = 0.998 \text{ g}/\text{cm}^3$), w is the mass of the moist wood sample, and w_0 is the mass of the wood sample after drying at $110 \text{ }^\circ\text{C}$ for 1 day using an electric oven. For the wood samples in this work, the difference between the water density calculated from the mass and the water density of a cross section measured by a moisture meter was $\Delta\rho_{\text{wat}} = 0.03 \text{ g}/\text{cm}^3$. Note that the specific gravity of the wood sample after drying at $110 \text{ }^\circ\text{C}$ for 1 day was $0.65 \pm 0.01 \text{ g}/\text{cm}^3$.

The complex permittivity of the wood samples was measured in the frequency range of 40 Hz to 10 GHz at room temperature ($25 \pm 3 \text{ }^\circ\text{C}$) and room humidity ($45 \pm 5\% \text{RH}$). We used two sets of dielectric measurement equipment to cover a wide frequency range. From 100 MHz to 10 GHz, time-domain reflectometry (TDR) measurements were carried out [34, 35]. We performed improved TDR measurements using a communication signal analyzer (CSA8200, Tektronix) with an 80E04 sampling module. For measurements from 40 Hz to 110 MHz, an impedance analyzer (4294A, Agilent) was used. The diameters of the outer conductor and center conductor of the flat-end coaxial electrode used for TDR measurements were 2.6 and 0.6 mm, and those for

the impedance measurements were 6.4 and 1.8 mm, respectively. When the dielectric measurements of wood samples are performed in the longitudinal, radial, and tangential directions, anisotropy of the dielectric constant is often observed [36–38]. In this work, the flat-end coaxial electrodes were placed in contact with the cross section of the wood samples, and dielectric measurements were performed in the longitudinal direction (i.e., the fiber direction). The dielectric measurements of the wood samples were carried out under nonequilibrium states because the dielectric measurements were carried out in a drying process of the wood samples. The measurement time of the TDR measurements and the impedance measurements was 1 min. The difference in the water density before and after measurements was lower than $0.01 \text{ g}/\text{cm}^3$ even when dielectric measurements were carried out several times to confirm the plasticity of the data. The effective depth of the electrical field of the flat-end electrode used for TDR measurements was 1 mm, and the dielectric spectrum reflected the averaged dynamics of the water within this electrical field depth [31–33].

Results and discussion

Figures 1 and 2 show the dielectric spectra of the sapwood of *Zelkova serrata* with various water densities measured in the fiber direction. A dielectric loss peak is observed in the GHz region, whose amplitude

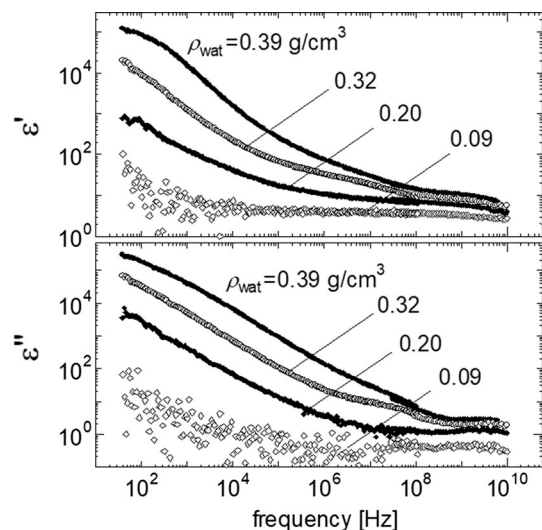


Figure 1 Dielectric spectra of *Zelkova serrata* with various water densities measured in the fiber direction.

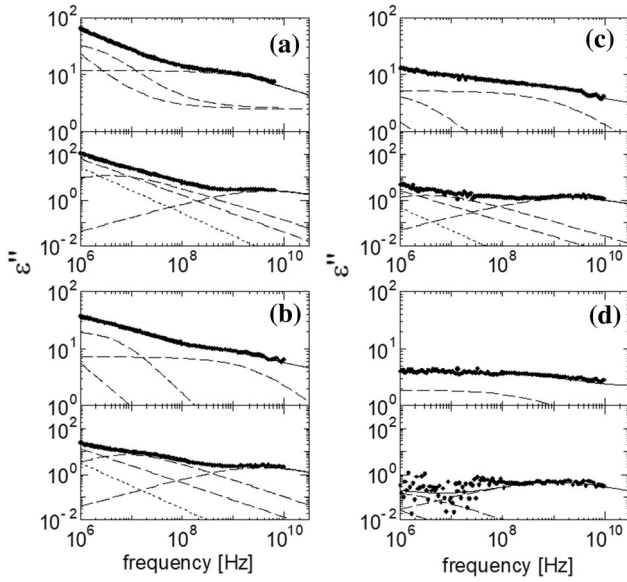


Figure 2 Dielectric loss spectra of *Zelkova serrata* measured in the fiber direction. **a** $\rho_{\text{wat}} = 0.39 \text{ g/cm}^3$, **b** 0.32, **c** 0.20, **d** 0.09. The dashed line indicates the loss spectrum calculated by the Cole–Cole equation. The dotted line indicates the term corresponding to the conductivity contribution. The solid line indicates the simple summation of the Cole–Cole equations and the conductivity contribution calculated by Eq. 2.

decreases with decreasing water density. A large contribution of the conductivity is observed below 100 MHz, which also decreases with decreasing water density. To clarify the dielectric properties of the relaxation process in the GHz region, we performed a curve-fitting procedure for the dielectric spectra using a summation of the Cole–Cole equations and a term representing the dc conductivity as follows:

$$\varepsilon^*(\omega) = \varepsilon' - j\varepsilon'' = \varepsilon_\infty + \sum_{i=0}^3 \frac{\Delta\varepsilon_i}{1 + (j\omega\tau_i)^{\beta_{CCi}}} + \frac{\sigma}{j\omega\varepsilon_0}. \quad (2)$$

Here, ε' is the dielectric constant, ε'' is the dielectric loss, j is the imaginary unit, ε_∞ is the limiting high-frequency permittivity, $\Delta\varepsilon$ is the relaxation strength, ω is the angular frequency, τ is the relaxation time, σ is the dc conductivity, and ε_0 is the permittivity of free space. β_{CC} ($0 < \beta_{CC} \leq 1$) is the relaxation time distribution reflecting the symmetric extension of the loss spectrum. Each spectrum is well described by the relaxation curve calculated using Eq. 2 as shown in Fig. 2. The relaxation process observed in the GHz region is named process *I*, and we focus on the water density dependence of the dielectric behavior of process *I*.

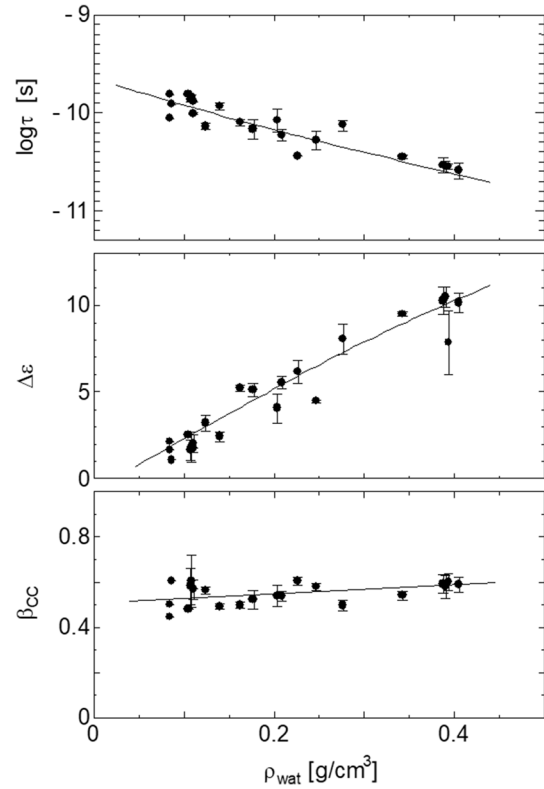


Figure 3 Plots of the relaxation time, relaxation strength, and relaxation time distribution against water density for *Zelkova serrata*.

Figure 3 shows the water density dependence of the dielectric parameters of process *I*. The relaxation strength linearly increases with increasing water density. The relaxation time decreases with increasing water density and approaches the relaxation time of bulk water ($\tau = 8.3 \text{ ps}$) [39]. These results indicate that process *I* reflects the molecular dynamics of water in wood. Note that β_{CC} increases slightly with increasing water density. We previously reported that the dielectric behavior of the relaxation processes reflects the motion of free water and bound water in various moist materials [25–30]. The relaxation time of the relaxation process of free water observed in these moist materials was 8–40 ps. On the other hand, the relaxation time of the relaxation process of bound water is more than 100 times longer than that of the relaxation process of free water. The relaxation time of process *I* observed in wood is close to that of the relaxation process of free water observed in these moist materials. Note that the relaxation processes of the bound water in *Zelkova serrata* exist in the frequency range in which the contribution of the ionic conductivity is observed, where the behavior of the

relaxation processes of the bound water is reported in Ref. [33]. In this work, the molecular dynamics of water leading to process *I* is clarified.

The relaxation strength is related to the local environment of the dipole moment, such as the dipole moment density and the arrangement of the dipole moments. It is generally accepted that water molecules in the liquid state form a tetrahedral local structure by hydrogen bonding, which is similar to the structure of ice. If the arrangement of water in a moist material remains the tetrahedral local structure, the ideal relaxation strength, $\Delta\epsilon_{ideal}$, will have a linear relationship with the water density. Thus, the ideal relaxation strength of water in wood is calculated and compared with the experimental value, $\Delta\epsilon_{exp}$. The straight dashed line in Fig. 4 indicates the ideal relaxation strength of free water, which connects the relaxation strength of 73.2 for pure water at $\rho_{wat} = 0.994 \text{ g/cm}^3$ and that of 0 at $\rho_{wat} = 0 \text{ g/cm}^3$ [39]. $\Delta\epsilon_{exp}$ is smaller than $\Delta\epsilon_{ideal}$ in the entire water density range measured, and the gradient of the line for $\Delta\epsilon_{exp}$ is one-third of that for $\Delta\epsilon_{ideal}$. These results can be interpreted to mean that part of the water molecules in wood contribute to process *I*. Other water molecules behave as bound water, and these water molecules contribute to the relaxation processes existing in the frequency range lower than that of process *I* [33]. The number of water molecules contributing to process *I* linearly increases with increasing water density of wood. These water molecules form the tetrahedral local structure through the hydrogen bonds, and a marked change in this local structure does not occur in the entire

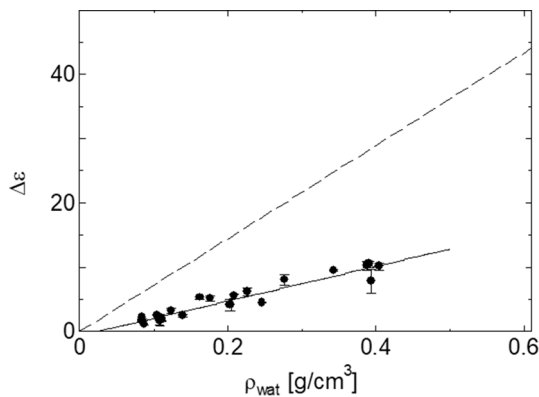


Figure 4 Plots of the relaxation strength in the relaxation process due to the motion of free water against the water density. The dashed line connects the relaxation strength of 73.2 for pure water at $\rho_{wat} = 0.994 \text{ g/cm}^3$ and that of 0 at $\rho_{wat} = 0 \text{ g/cm}^3$.

water density range measured. Note that the relaxation strength reaches $\Delta\epsilon_{exp} = 0$ at $\rho_{wat} = 0.03 \text{ g/cm}^3$. This result indicates that the water molecules contributing to process *I* are completely desorbed below $\rho_{wat} = 0.03 \text{ g/cm}^3$.

For moist materials, a very large dielectric loss is often observed in the low-frequency range of the dielectric loss spectrum, and this behavior is interpreted to correspond to ionic conduction in the medium. The ionic conductivity can be described as $\sigma = nz\mu$, where n is the ion density, z is the ion charge, and μ is the ion mobility. To discuss the relationship between the amount of water and the ionic conductivity, Fig. 5 shows plots of the dielectric loss observed at 100 Hz, $\epsilon''_{100\text{Hz}}$, against the water density of wood. $\epsilon''_{100\text{Hz}}$ decreases with decreasing water density. The water density dependence of $\epsilon''_{100\text{Hz}}$ can be described as

$$\epsilon''_{100\text{Hz}} = \epsilon''_c (\rho_{wat} - \rho_c)^k, \tag{3}$$

where ϵ''_c , k , and ρ_c are empirical parameters. ρ_c can be considered as the threshold water density at which ionic conduction starts to occur. Table 1 shows the empirical parameters of Eq. 3 calculated by least-squares curve fitting. The value of ρ_c ($= 0.05 \text{ g/cm}^3$) is in good agreement with the water density at which the relaxation strength of process *I* reaches $\Delta\epsilon_{exp} = 0$ as shown in Fig. 4. These results indicate that the water contributing to process *I* behaves as a water path that transports ions, and the ionic conductivity decreases with decreasing water density caused by the breakage of the water path.

Process *I* observed in wood reflects the molecular dynamics of water, and the dielectric spectrum of this process has the Cole–Cole-type distribution. The

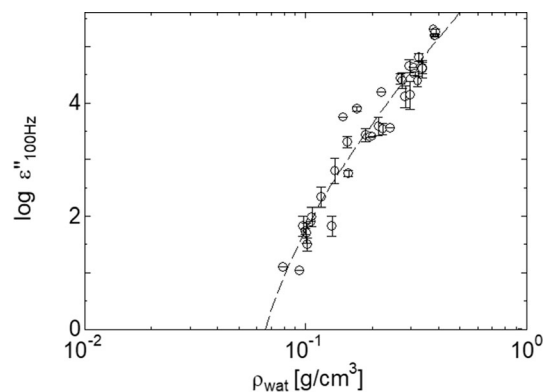


Figure 5 Plots of the logarithm of the dielectric loss against the water density. The dashed line is calculated by Eq. 3.

Table 1 Parameters obtained by analysis using Eq. 3

p_c	ε''_c	K
0.04	1.13×10^7	4.3

Cole–Cole-type relaxation process has also been observed for the relaxation process of free water in synthetic polymer–water and biopolymer–water mixtures [25–30, 32] and for the relaxation process of molecular liquids confined in porous systems [31, 40, 41]. In the experimental results for these polymer–water mixtures, the dielectric relaxation time of the relaxation process reflecting the molecular dynamics of water increases, and the relaxation time distribution indicating the broadness of the symmetric loss peak decreases with decreasing water content [25–30, 32]. These water content dependences of the relaxation time and time distribution can be explained by the geometrical self-similarity of a polymer network using a geometrical parameter called the space fractal dimension, d_G , as follows: [42]

$$\beta_{CC} = \frac{d_G \ln(\tau\omega_S)}{2 \ln(\tau/\tau_0)}. \quad (4)$$

Here, τ_0 is the cutoff time of the scaling in time. ω_S is the characteristic frequency of the self-diffusion process associated with the self-diffusion coefficient of water, and ω_S is related to the average self-diffusion constant, D_S , as $\omega_S \sim 2d_E D_S/R_0^2$. Here, R_0 is the cutoff size of the scaling in the space or the size of the cooperative domain. When water molecules form a cooperative domain via hydrogen bonds, the scaling cutoff size in the space can be treated as the size of a water molecule of 3 Å. d_E is the Euclidean dimension. When water molecules diffuse, the Euclidean dimension can be assumed to be $d_E = 2$. According to the above expressions, the molecular dynamics of water under a geometric constraint can be discussed by considering the $\tau - \beta_{CC}$ diagram [25–30, 42]. In the $\tau - \beta_{CC}$ diagram for the relaxation process in confined systems, plots are located at a larger τ and smaller β_{CC} for stronger interactions between the relaxation units and statistical confinement.

Figure 6 shows a $\tau - \beta_{CC}$ diagram for process I in *Zelkova serrata* with various water densities. The plots in the $\tau - \beta_{CC}$ diagram can be described by Eq. 4. Table 2 shows the empirical parameters of Eq. 4 calculated by least-squares curve fitting. The space fractal dimension d_G is slightly larger than unity. We have already performed dielectric measurements for

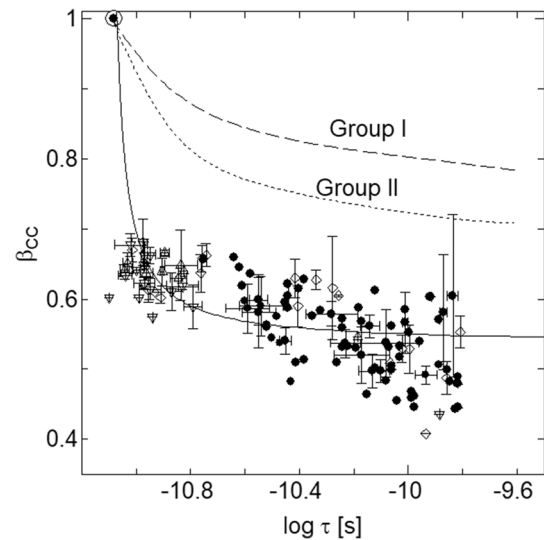


Figure 6 $\tau - \beta_{CC}$ diagram for different species of wood. Closed circles: sawwood of *Zelkova serrata*, double circle: pure water, open diamonds: sawwood of *Cornus controversa*, open triangles: sawwood of *Cryptomeria japonica*, open downward triangles: heartwood of *Cryptomeria japonica*. The dashed line is calculated by Eq. 4.

the deciduous tree *Cornus controversa* and the evergreen needle-leaved tree *Cryptomeria japonica*. The plots in the $\tau - \beta_{CC}$ diagram for these different species of wood show good agreement as shown in Fig. 6. These results indicate that the dynamical local structure formed by the water in wood shows similar self-similarity, and this feature is independent of the wood species. We have already reported the $\tau - \beta_{CC}$ diagram for various polymer–water mixtures. These $\tau - \beta_{CC}$ diagrams can be classified into two groups [42–44]: Group I comprises hydrophobic polymers, such as poly(ethylene glycol), poly(vinyl methyl ether), and moist collagen, whereas group II comprises hydrophilic polymers, such as poly(acrylic acid), poly(ethylenimine), poly(allylamine), poly(vinyl alcohol), and gelatin. The $\tau - \beta_{CC}$ diagram for process I observed in wood markedly deviates from these two groups, and the fractal parameters d_G , ω_S , and D_S for the water in wood are much smaller than those in the polymer–water mixtures as shown in Table 2. Next, we discuss the molecular descriptions of water in wood based on the fractal descriptions.

The space fractal dimension has been widely used to describe geometric patterns showing self-similarity in various natural phenomena. A characteristic fractal dimension slightly larger than unity has been observed in some natural phenomena [45–49]. In the

Table 2 Parameters obtained by fractal analysis using Eq. 4 for wood sample (in this work) and polymer–water mixtures (reported in Ref. [42])

	d_G	ω_s (Hz)	τ_0 (s)	D_s (m ² /s)
<i>Zelkova serrata</i>	1.1	1.4×10^{11}	7.8×10^{-12}	3.2×10^{-9}
Poly(ethylene glycol)	1.5	2.8×10^{11}	4.5×10^{-12}	6.3×10^{-9}
Poly(vinyl methyl ether)	1.4	4.2×10^{11}	3.6×10^{-12}	9.5×10^{-9}
Poly(acrylic acid)	1.1	2.1×10^{11}	6.3×10^{-12}	4.7×10^{-9}
Poly(ethylenimine)	1.3	2.7×10^{11}	4.9×10^{-12}	6.1×10^{-9}

penetration phenomena of a liquid, when a low-viscosity fluid (such as water) penetrates into a high-viscosity fluid (such as oil) upon applying a high pressure, the low-viscosity fluid exhibits instability and divides into branches in the direction perpendicular to that of the compression. This characteristic branch formation can be considered to exhibit self-similarity, and the fractal dimension of the apparent length of the branch patterns is 1.12 [46]. In molecular science, the geometric pattern of a kinetic growth process, such as the polymerization and aggregation of colloids and clusters, has been evaluated using various scattering methods. The spatial distribution of linear chains and chainlike clusters formed by rigid particles with a small number of branches shows self-similarity, and its fractal dimension is about 1.2–1.4 [47–49]. These results indicate that when particles are corrected in the length direction and the corrected particles form some branches, the particles show self-similarity and the fractal dimension is slightly larger than unity.

It is generally accepted that water molecules form a tetrahedral hydrogen-bonded network structure. The water molecules in pure water cooperatively move owing to the hydrogen bonding, and this cooperative dynamics leads to the Debye-type relaxation process observed in the GHz region. On the other hand, polymer chains in polymer–water mixtures form a random coil conformation. This conformation depends on the molecular structure of the polymer and is characterized by self-similarity [42–44]. The cooperative dynamics of water restricted by the conformation of the polymer chain leads to the Cole–Cole-type relaxation process. Thus, the $\tau - \beta_{CC}$ diagram obtained from the Cole–Cole-type relaxation process is characterized by the self-similarity of polymer chains, and the fractal dimension obtained from the $\tau - \beta_{CC}$ diagram depends on the molecular structure of the polymer as shown in Table 2 [42–44]. Note that even values smaller than unity have been reported for aqueous dispersion systems such as

globular proteins and foodstuffs in which the hydrogen-bonded network structure of water molecules is fractionated by dispersion particles [31]. Thus, the molecular dynamics of water contributing to process *I* in wood can also be interpreted on the basis of fractal descriptions. The water molecules contributing to process *I* exist inside the void spaces such as the intercellular spaces, lumens, tracheids, and vessels. Around $\rho_{\text{wat}} = 0.03 \text{ g/cm}^3$, the water molecules form the tetrahedral hydrogen-bonded structure, which is fractionated on the inner walls of the void spaces. The size of the hydrogen-bonded structure grows along the inner walls of void spaces through the absorption of water molecules with increasing water density. Then, this growth of the network structure is dominant in the length direction, and the gradient of the line for $\Delta\epsilon_{\text{exp}}$ is smaller than that for $\Delta\epsilon_{\text{ideal}}$ as shown in Fig. 4. The molecular dynamics of these water molecules is strongly restricted between the inner walls of the void spaces and air spaces. This strongly restricted molecular dynamics of water in wood leads to the marked deviation of the $\tau - \beta_{CC}$ diagram from the results obtained for polymer–water mixtures.

The water density can be used to interpret the dielectric parameters as a function of the water content, because the dielectric relaxation strength is proportional to the water density as shown in Fig. 4. However, the moisture content (MC) has conventionally been used to describe the water content of wood, which is given by

$$\text{MC} = \frac{w - w_0}{w_0}. \quad (5)$$

The fiber saturation point expressed in terms of MC is defined as the water content at which the free water has been completely removed. The fiber saturation point does not depend on the wood species and is at MC = 30%. Below the fiber saturation point, the moisture transportation and electrical properties of wood have been interpreted in terms of bound water diffusion and vapor water diffusion [50–54]. The

water density at which the relaxation strength of process *I* vanishes as shown in Fig. 4 is equivalent to the moisture content $MC = 3\%$, and this water content is much lower than the fiber saturation point. To consider the relationship between the water molecules contributing to process *I* and the water molecules in vapor, dielectric measurements of wood were performed under a helium environment. First, TDR measurements of wood samples whose water density reached $\rho_{\text{wat}} = 0.05 \text{ g/cm}^3$ were performed in an air environment at 47%RH. The observed relaxation strength of process *I* was 1.0. Next, these wood samples were placed inside a helium chamber at 1%RH, and TDR measurements of the wood samples were performed in flowing helium. Process *I* was also observed in the wood after flowing helium for 3 h as shown in Fig. 7. The relaxation strength of process *I* was observed to decrease to lower than 0.3, while the water density slightly decreased ($\rho_{\text{wat}} = 0.04 \text{ g/cm}^3$) upon placing the wood samples in a helium environment. These results indicate that the relaxation strength of process *I* strongly depends on the amount of water vapor around the wood samples. However, the number of water molecules per unit volume of vapor is very small, and the dielectric constant of vapor is 1.0 [55]. On the other hand, the relaxation strength of process *I* observed in the wood increased with increasing water density

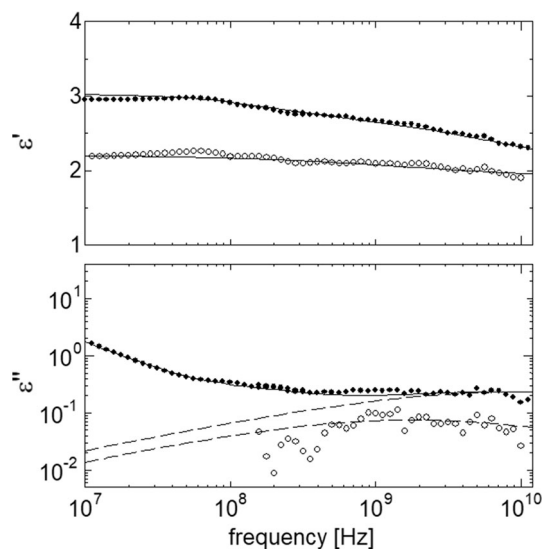


Figure 7 Dielectric spectra of *Zelkova serrata* measured along the fiber direction. ●: dielectric spectrum of wood sample measured by TDR method at 25 °C in air environment at 47%RH, ○: dielectric spectrum of wood sample measured by TDR method at 25 °C in helium environment at 1%RH.

reaching 5.0 around the fiber saturation point ($\rho_{\text{wat}} = 0.23 \text{ g/cm}^3$). The water contributing to process *I* observed in the wood is interpreted as follows. In accordance with the results reported in Refs. [50–54], we assumed that bound water and water vapor exist in wood below the fiber saturation point. Our experimental results suggest that the water molecules in vapor repeatedly undergo adsorption and desorption on the inner walls of the void spaces, and then the adsorbed water molecules form the local structure leading to process *I*.

Conclusion

We performed dielectric measurements of wood along the fiber direction in the frequency range of 40 Hz to 10 GHz using flat-end coaxial electrodes. The Cole–Cole-type relaxation process (process *I*) reflecting the molecular dynamics of the water in the wood was observed in the GHz region. The water density dependences of the relaxation time and strength of process *I* are similar to those of the relaxation process of free water observed in polymer–water mixtures. However, the $\tau - \beta_{\text{CC}}$ diagram of process *I* markedly deviates from that of the relaxation process of free water in polymer–water mixtures. The molecular dynamics of the water contributing to process *I* observed in wood is interpreted as follows. Part of the water molecules in the vapor adhere to the inner walls of the void spaces, and these water molecules form the local structure leading to process *I*. These local structures are fractionated on the inner walls of the void spaces, and the size of the local structure grows in the length direction along the walls of void spaces with increasing water density. The molecular dynamics of these water molecules is strongly restricted between the inner walls of the void spaces and air spaces. This strongly restricted molecular dynamics of water in wood leads to the marked deviation of the $\tau - \beta_{\text{CC}}$ diagram from the results obtained for polymer–water mixtures. The water density dependence of the dielectric relaxation parameters of process *I* observed in wood shows a continuous change around the fiber saturation point. This result indicates that the adsorbed water molecules from the vapor concentrate locally and form the local structure, and the dynamical behavior of these water molecules continuously changes to that of free water.

Compliance with ethical standards

Conflict of interest The authors declare no conflict of interest.

References

- [1] Skaar C (1988) Wood-water relations. Springer, Berlin
- [2] Zelinka SL, Lambrecht MJ, Glass SV, Wiedenhoft AC, Yelle DJ (2012) Examination of water phase transitions in Loblolly pine and cell wall components by differential scanning calorimetry. *Thermochim Acta* 533:39–45
- [3] Simpson W (1980) Sorption theories applied to wood. *Wood Fiber Sci* 12:183–195
- [4] Labbé N, Jéso BD, Lartigue JC, Daudé G, Pétraud M, Ratier M (2006) Time-domain 1H NMR characterization of the liquid phase in greenwood. *Holzforchung* 60:265–270
- [5] Telkki VV, Yliniemi M, Jokisaari J (2013) Moisture in softwoods: fiber saturation point, hydroxyl site content, and the amount of micropores as determined from NMR relaxation time distributions. *Holzforchung* 67:291–300
- [6] Yang SY, Eom CD, Han Y, Chang Y, Park Y, Lee JJ, Choi JW, Yeo H (2014) Near-Infrared spectroscopic analysis for classification of water molecules in wood by a theory of water mixtures. *Wood Fiber Sci* 46:138–147
- [7] Jinzhen C, Guangjie Z (2001) Dielectric relaxation based on adsorbed water in wood cell wall under non-equilibrium state 2. *Holzforchung* 55:87–92
- [8] Sugimoto H, Norimoto M (2004) Dielectric relaxation due to interfacial polarization for heat-treated wood. *Carbon* 42:211–218
- [9] Sugimoto H, Takazawa R, Norimoto M (2005) Dielectric relaxation due to heterogeneous structure in moist wood. *J Wood Sci* 51:549–553
- [10] Sugimoto H, Norimoto M (2005) Dielectric relaxation due to the heterogeneous structure of wood charcoal. *J Wood Sci* 51:554–558
- [11] Wang Y, Minato K, Iida I (2008) Mechanical properties of wood in an unstable state due to temperature changes, and analysis of the relevant mechanism VI: dielectric relaxation of quenched wood. *J Wood Sci* 54:16–21
- [12] Le BD, Strømme M, Mihranyan A (2015) Characterization of dielectric properties of nanocellulose from wood and algae for electrical insulator applications. *J Phys Chem B* 119:5911–5917
- [13] Rawat SPS, Khali DP (1998) Clustering of water molecules during adsorption of water in wood. *J Polym Sci B* 36:665–671
- [14] Runt JP, Fitzgerald JJ (1997) Dielectric spectroscopy of polymeric materials. American Chemical Society, New York
- [15] Kremer F, Schönhals A (2003) Broadband dielectric spectroscopy. Springer, Berlin
- [16] Jinzhen C, Guangjie Z (2002) Dielectric relaxation based on adsorbed water in wood cell wall under non-equilibrium state. Part 3: Desorption. *Holzforchung* 56:655–662
- [17] Sugiyama M, Norimoto M (2006) Dielectric relaxation of water adsorbed on chemically treated woods. *Holzforchung* 60:549–557
- [18] Sugimoto H, Kanayama K, Norimoto M (2007) Dielectric relaxation of water adsorbed on wood and charcoal. *Holzforchung* 61:89–94
- [19] Handa T, Fukuoka M, Yoshizawa S, Kanamoto T (1982) The effect of moisture on the dielectric relaxations in wood. *J Appl Polym* 27:439–453
- [20] Mai TC, Razafindratsima S, Sbartai ZM, Demontoux F, Bos F (2015) Non-destructive evaluation of moisture content of wood material at GPR frequency. *Constr Build Mater* 77:213–217
- [21] Koubaa A, Perré P, Hutcheon RM, Lessard J (2008) Complex dielectric properties of the sapwood of aspen, white birch, yellow birch, and sugar maple. *Dry Technol* 26:568–578
- [22] Tomppo L, Tiitta M, Laakso T, Harju A, Venäläinen M, Lappalainen R (2009) Dielectric spectroscopy of scots pine. *Wood Sci Technol* 43:653–667
- [23] Jördens C, Wietzke S, Scheller M, Koch M (2010) Investigation of the water absorption in polyamide and wood plastic composite by terahertz time-domain spectroscopy. *Polym Test* 29:209–215
- [24] Bossou OV, Mosig JR, Zurcher JF (2010) Dielectric measurements of tropical wood. *Measurement* 43:400–405
- [25] Shinyashiki N, Sudo S, Abe W, Yagihara S (1998) Shape of dielectric relaxation curves of ethylene glycol oligomer-water mixtures. *J Chem Phys* 109:9843–9847
- [26] Shinyashiki N, Yagihara S, Arita I, Mashimo S (1998) Dynamics of water in a polymer matrix studied by a microwave dielectric measurement. *J Phys Chem B* 102:3249–3258
- [27] Shinyashiki N, Yagihara S (1999) Comparison of dielectric relaxations of water mixtures of poly(vinylpyrrolidone) and 1-vinyl-2-pyrrolidinone. *J Phys Chem B* 103:4481–4484
- [28] Yagihara S, Oyama M, Inoue A, Asano M, Sudo S, Shinyashiki N (2007) Dielectric relaxation measurement and analysis of restricted water structure in rice kernels. *Meas Sci Technol* 18:983–990
- [29] Hayashi Y, Shinyashiki N, Yagihara S (2002) Dynamical structure of water around biopolymers investigated by

- microwave dielectric measurements via time domain reflectometry. *J Non Cryst Solids* 305:328–332
- [30] Hayashi Y, Oshige I, Katsumoto Y, Omori S, Yasuda A (2007) Protein–solvent interaction in urea–water systems studied by dielectric spectroscopy. *J Non Cryst Solids* 353:4492–4496
- [31] Yagihara S, Miura N, Hayashi Y, Miyairi H, Asano M, Yamada G, Shinyashiki N, Mashimo S, Umehara T, Tokita M, Naito S, Nagahama T, Shiotsubo M (2001) Microwave dielectric study on water structure and physical properties of aqueous systems using time domain reflectometry with flat-end cells. *Subsurf Sens Technol Appl* 2:15–29
- [32] Yagihara S (2015) Nano/micro science and technology in biorheology: principles. In: Dobashi T, Kita R (eds) *Methods, and applications*. Springer, Tokyo, pp 183–213
- [33] Abe F, Nishi A, Saito H, Asano M, Watanabe S, Kita R, Shinyashiki N, Yagihara S, Fukuzaki M, Sudo S, Suzuki Y (2017) Dielectric study on hierarchical water structures restricted in cement and wood materials. *Meas Sci Technol* 28:044008–044017
- [34] Cole RH, Mashimo S, Winsor PJ IV (1980) Evaluation of dielectric behavior by time domain spectroscopy. 3. Precision difference methods. *J Phys Chem* 84:786–793
- [35] Mashimo S, Umehara T, Ota T, Kuwabara S, Shinyashiki N, Yagihara S (1987) Evaluation of complex permittivity of aqueous solution by time domain reflectometry. *J Mol Liq* 36:135–151
- [36] Norimoto M, Hayashi S, Yamada T (1978) Anisotropy of dielectric constant in coniferous wood. *Holzforschung* 32:167–172
- [37] Kabir MF, Daud WM, Khalid K, Sidek HAA (1998) Dielectric and ultrasonic properties of rubber wood. Effect of moisture content grain direction and frequency. *Eur J Wood Wood Prod* 56:223–227
- [38] Sahin H, Ay N (2004) Dielectric properties of hardwood species at microwave frequencies. *J Wood Sci* 50:375–380
- [39] Barthel J, Bachhuber K, Buchner R, Hetzenauer H (1990) Dielectric spectra of some common solvents in the microwave region. Water and lower alcohols. *Chem Phys Lett* 165:369–373
- [40] Schüller J, Melnichenko YB, Richert R, Fischer EW (1994) Dielectric studies of the glass transition in porous media. *Phys Rev Lett* 73:2224–2227
- [41] Schüller J, Richert R, Fischer EW (1995) Dielectric relaxation of liquids at the surface of a porous glass. *Phys Rev B* 52:15232–15238
- [42] Ryabov YE, Feldman Y, Shinyashiki N, Yagihara S (2002) The symmetric broadening of the water relaxation peak in polymer–water mixtures and its relationship to the hydrophilic and hydrophobic properties of polymers. *J Chem Phys* 116:8610–8615
- [43] Kundu SK, Yagihara S, Yoshida M, Shibayama M (2009) Microwave dielectric study of an oligomeric electrolyte gelator by time domain reflectometry. *J Phys Chem B* 113:10112–10116
- [44] Kundu SK, Okudaira S, Kosuge M, Shinyashiki N, Yagihara S (2009) Phase transition and abnormal behavior of a nematic liquid crystal in benzene. *J Phys Chem B* 113:11109–11114
- [45] Martin JE, Hurd AJ (1987) Scattering from fractals. *J Appl Cryst* 20:61–78
- [46] Nittmann J, Daccord G, Stanley HE (1985) Fractal growth of viscous fingers: quantitative characterization of a fluid instability phenomenon. *Nature* 314:141–144
- [47] Zhang SW (1998) State-of-the-art of polymer tribology. *Tribol Int* 31:49–60
- [48] Augé S, Schmit PO, Crutchfield CA, Islam MT, Harris DJ, Durand E, Clemancey M, Quoineaud AA, Lancelin JM, Prigent Y, Taulelle F, Delsuc MA (2009) NMR measure of translational diffusion and fractal dimension. Application to molecular mass measurement. *J Phys Chem B* 113:1914–1918
- [49] Takahashi A, Kita R, Shinozaki T, Kubota K, Kaibara M (2003) Real space observation of three-dimensional network structure of hydrated fibrin gel. *Colloid Polym Sci* 281:832–838
- [50] Gezici-Koç Ö, Erich SJF, Huinink HP, van der Ven LGJ, Adan OCG (2017) Bound and free water distribution in wood during water uptake and drying as measured by 1D magnetic resonance imaging. *Cellulose* 24:535–553
- [51] Eitelberger J, Hofstetter K, Dvinskikh SV (2011) A multi-scale approach for simulation of transient moisture transport processes in wood below the fiber saturation point. *Compos Sci Technol* 71:1727–1738
- [52] Jia D, Afzal MT (2008) Modeling the heat and mass transfer in microwave drying of white oak. *Dry Technol* 26:1103–1111
- [53] Kang W, Kang CW, Chung WY, Eom CD, Yeo H (2008) The effect of openings on combined bound water and water vapor diffusion in wood. *J Wood Sci* 54:343–348
- [54] Han Y, Park JH, Chang YS, Eom CD, Lee JJ, Yeo H (2013) Classification of the conductance of moisture through wood cell components. *J Wood Sci* 59:469–476
- [55] Uematsu M, Frank EU (1980) Static dielectric constant of water and steam. *J Phys Chem Ref Data* 9:1291–1306